Water Research 233 (2023) 119791

Contents lists available at ScienceDirect

Water Research

journal homepage: www.elsevier.com/locate/watres

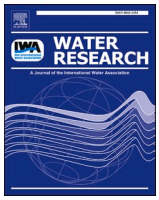

# Wildfire effects on the hydrogeochemistry of a river severely polluted by acid mine drainage

Jonatan Romero-Matos *, Carlos R. Cánovas, Francisco Macías, Rafael Pérez-López, Rafael León, Ricardo Millán-Becerro, Jose Miguel Nieto

*Department of Earth Sciences & Research Center on Natural Resources, Health and the Environment. University of Huelva, Campus "El Carmen", 21071, Huelva, Spain*

ARTICLE INFO

*Keywords:*
Mining pollution
Seasonal variations
Natural attenuation
Ash
Evaporitic salts washout
Climate change

ABSTRACT

This study evaluates for the first time the impact of a large wildfire on the hydrogeochemistry of a deeply AMD-affected river at the beginning of the wet season. To accomplish this, a high-resolution water monitoring campaign was performed within the basin coinciding with the first rainfalls after summer. Unlike similar events recorded in AMD-affected areas, where dramatic increases in most dissolved element concentrations, and decreases in pH values are observed as a result of evaporitic salts flushing and the transport of sulfide oxidation products from mine sites, a slight increase in pH values (from 2.32 to 2.88) and decrease in element concentrations (e.g.; Fe: 443 to 205 mg/L; Al: 1805 to 1059 mg/L; sulfate: 22.8 to 13.3 g/L) was observed with the first rainfalls after the fire. The washout of wildfire-ash deposited in the riverbanks and the drainage area, constituted by alkaline mineral phases, seems to have counterbalanced the usual behavior and patterns of the river hydrogeochemistry during autumn. Geochemical results indicate that a preferential dissolution occurs during ash washout (K > Ca > Na), with a quick release of K followed by an intense dissolution of Ca and Na. On the other hand, in unburnt zones parameters and concentrations vary to a lesser extent than burnt areas, being the washout of evaporitic salts the dominant process. With subsequent rainfalls ash plays a minor role on the river hydrochemistry. Elemental ratios ($Fe/SO_4$ and Ca/Mg) and geochemical tracers in both ash (K, Ca and Na) and AMD (S) were used to prove the importance of ash washout as the dominant geochemical process during the study period. Geochemical and mineralogical evidences point to intense schwertmannite precipitation as the main driver of reduction in metal pollution. The results of this study shed light on the response of AMD-polluted rivers to certain climate change effects, since climate models predict an increase in the number and intensity of wildfires and torrential rain events, especially in Mediterranean climates.

## 1. Introduction

Acid mine drainage (AMD) constitutes one of the most severe cases of worldwide water pollution given its extreme acid load generated after intense sulfide oxidation processes (Nordstrom et al., 2015). These processes may irreversibly worsen the conditions of the receiving watercourses for a long-term, even hundreds to thousands of years after the cease of the mining activity (Younger, 1997). The Odiel and Tinto watersheds (Huelva province, SW Spain) are globally recognized examples of AMD pollution due to the low pH values and extreme metal(loid)s and sulfate concentrations observed in their waters, as a result of the contribution of numerous discharges of acidic leachates from historically mined massive sulfide deposits (Cánovas et al., 2021). River discharge and hydrogeochemistry vary seasonally, with maximum pollutant concentrations during the first rainfalls of autumn, caused by the washout of efflorescent salts that commonly precipitate during the dry season, and minimum concentrations of pollutants during large flood events by runoff dilution processes (e.g., Cánovas et al., 2017; Olías et al., 2020). However, these conditions may change upon certain causes such as mine spills (e.g., Olías et al., 2019), the adoption of remediation measures (e.g., Macías et al., 2017; Wang et al., 2019), and intentional or unintentional wildfires. In this latter case, it has been reported that wildfires may have significant effects on the water quality of fluvial catchments (e.g., Emelko et al., 2011; Emmerton et al., 2020; Pachecho and Fernandes, 2021).

In Mediterranean climates, such as that of Huelva province, wildfires are very common during the warm-dry season (e.g., Pausas, 2004; Pereira et al., 2005), due to high temperatures and absent of soil

* Corresponding author.
*E-mail address:* jonatan.romero@dct.uhu.es (J. Romero-Matos).

https://doi.org/10.1016/j.watres.2023.119791
Received 7 October 2022; Received in revised form 20 February 2023; Accepted 21 February 2023
Available online 24 February 2023

humidity. Their occurrence damages not only the terrestrial ecosystems but also affects the water bodies in a wide range. Wildfires may cause severe changes in physico-chemical properties of soils, increasing the erosion rates and run-off generation capacity which may modify sediment fluxes, nutrients and other water constituents (Smith et al., 2011; Bladon et al., 2014). On the one hand, riverflow and sediment fluxes may be altered by increased runoff generation induced by the clogging of soil pores by ash (Bodí et al., 2014), limiting the infiltration capacity of soils, and by the loss of vegetation and subsequent canopy interception, increasing the net precipitation (Williams et al., 2019). On the other hand, Pereira and Úbeda (2010) reported the release of heavy metals from wildfire-ash to soils and water bodies after a wildfire in a cork oak forest in NE Spain. Earl and Blinn (2003) observed increases in pH and alkalinity in stream waters following forest fires in SW of USA. While wildfire impacts on river and stream water quality have been certainly documented (e.g., Reale et al., 2015; Emelko et al., 2016; Rust et al., 2018; Mishra et al., 2021), their effects on the hydrogeochemistry of AMD-polluted rivers have not been previously studied.

The wildfire of Almonaster La Real (Huelva), which occurred in August-September 2020, burned during 12 days around 160 km$^2$ of forest in the surrounding areas of the Odiel River middle basin (Copernicus Emergency Management Service, 2020) (Fig. 1), which is intensively affected by AMD from abandoned mines. The continuous crown fire affected around 7.2% of the Odiel river basin, with a quick evolution (25 m/min) and burning rates from 4 to 10 km$^2$/h. Ash from burned regional vegetation (mostly *Pinus pinaster, Eucalyptus globulus, Quercus suber* and *Cistus ladanifer*) are highly alkaline, which may cause increases of water pH in soils by two to three units due to the solubilization of easily-soluble alkaline phases contained in them (Ulery et al., 1993; Pereira et al., 2011, 2014). Some of the inorganic compounds contained in the ash can form strong bases (i.e. Ca, Mg, Na and K) (Pereira and Úbeda, 2010; Gabet and Bookter, 2011). Silica is also a major

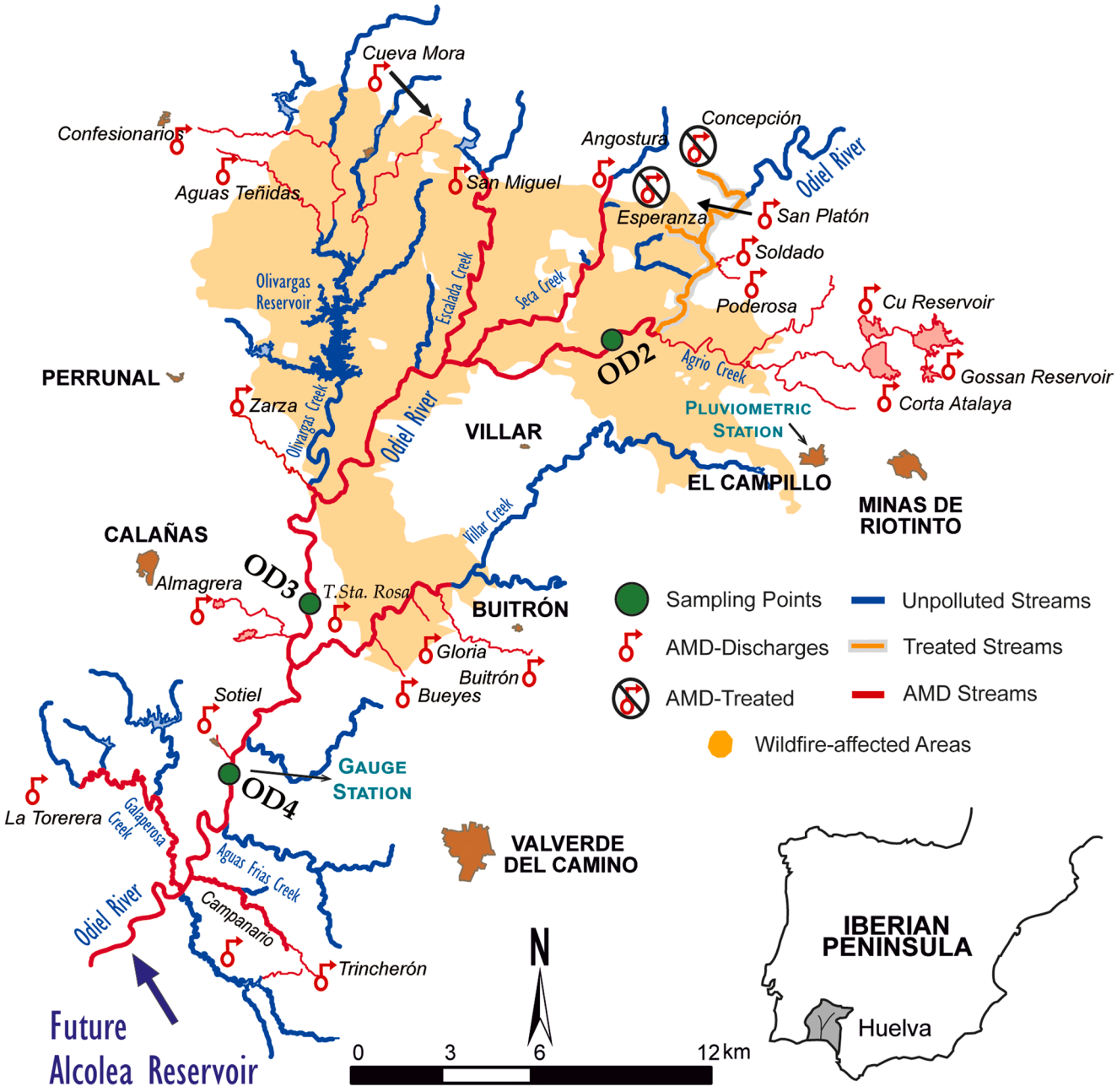


**Fig. 1.** Location map of the study area, showing the selected sampling points, rain and stream gauge stations, current AMD pollution of the watershed and the wildfire affected area, as well as the water courses where remediation actions have been performed.

component in ash with lower presence of other elements (e.g., P, S, Al, Fe, Mn and/or Zn) (Bodí et al., 2014). Audry et al. (2014) determined in plant litter ash that these elements are mainly hosted in soluble phases such as salts, carbonates and oxides depending on the combustion temperature. Due to their alkaline nature, the biomass ash has already been used as alkaline reagent for AMD treatment and other acidic leachates (e.g., Bogush et al., 2020; Millán-Becerro et al., 2021). On the assumption that this wildfire would have a significant impact on the Odiel River hydrogeochemistry, a sampling campaign was performed following the first rainfalls after the wildfire to evaluate the consequences of the soluble components of ash in the Odiel River. Therefore, the main goal of this paper is evaluating the influence of the wildfire-ash washout on the Odiel River hydrogeochemistry with the first rainfalls after the wildfire. These events will acquire growing importance as climate change predictions foresee that the expectations about the number and intensity of fires will increase worldwide in the future (Jolly et al., 2015; Kinoshita et al., 2016), driving such events to other AMD-sites and the influence reported in this work may be replicated. To our knowledge, this is the first study that tries to assess the effects of a wildfire on the hydrogeochemistry of an AMD-affected fluvial system.

## 2. Materials and methods

### 2.1. Sampling and analytical techniques

In order to study the effects of the wildfire on the Odiel River hydrogeochemistry following the first rainfalls after the cease of the Almonaster La Real wildfire, a sampling campaign was performed along the main watercourse (Fig. 1). The first point is located at the Cinco Ojos bridge (OD2), an area widely affected by the fire, which receives the AMD inputs from the Riotinto mines through the Agrio Creek, constituting around 40–60% of the total AMD pollution load of the Odiel River (Galván et al., 2016) and other minor AMD inputs (e.g., Poderosa, San Platón and Esperanza mines) located in the headwaters. Downstream, two different sampling points located outside of the fire-affected area were selected (Fig. 1): the Tinto-Santa Rosa bridge (OD3) and the Sotiel bridge (OD4), which receive (in addition to the abovementioned inputs) the influence of other minor abandoned mines (Fig. 1). The main mines that contribute to contamination at these points can be seen in Fig. 1. Flood events and the influence of washout processes on the Odiel River hydrochemistry has been previously studied at the sampling point OD4 due to the existence of a gauge station (Cánovas et al., 2012). The sampling was carried out during autumn 2020 (16/09/2020 - 02/12/2020). Samples were taken before, during and after rainy episodes ($n = 22$ for each sampling point) using pre-cleaned (with 10% $HNO_3$) bottles. Water samples were filtered with 0.22 μm cellulose nitrate filters. In total, 66 samples were collected, acidified to pH < 2 with $HNO_3$ suprapur and kept refrigerated until analysis. Different physicochemical parameters such as pH, electrical conductivity (EC) and oxidation–reduction potential (ORP) were measured in the field using a previously calibrated Crison MM40+ multiparameter probe (HACH LANGE GmbH, Düsseldorf, Germany). Calibration was conducted using standard solutions for pH (4.01, 7.00 and 9.21 at 25 °C), and EC (147 μS/cm, 1413 μS/cm and 12.88 mS/cm at 25 °C) while ORP was checked using 220 mV and 470 mV solutions at 25 °C. Redox potential measurements were corrected to standard hydrogen electrode (Nordstrom and Wilde, 1998).

Samples were analyzed at the Central Research Services of the University of Huelva by Inductively Coupled Plasma-Optical Emission Spectroscopy (ICP-OES; Jobin Yvon Ultima 2) for major elements. The detection limits were 200 μg/L for Al, Ca, Fe, K, Mg, Mn, Na, Si and S; 50 μg/L for Zn; and 5 μg/L for Cu. Triplicate analyses were performed to assess the analytical precision, which was below 5% (%RSD) in all samples. In each analysis sequence, control blanks were also analyzed, being the concentration of elements below the detection limits in each blank. The analytical accuracy was confirmed by the analysis of reference materials (NIST-1640). Dissolved $SO_4^{2-}$ concentrations were calculated from the total S concentrations, assuming that the presence of other S species was insignificant, which validity was checked using the geochemical code PHREEQC (Parkhurst and Appelo, 2013) and by comparison with values obtained by ion chromatography (IC) analysis (differences <5%).

Particulate matter retained in cellulose nitrate filters (0.22 μm porosity), and mineral assemblages formed by wildfire-ash coated with precipitated efflorescent salts, deposited in the river margin before the rainy events, were collected for mineralogical characterization. Thus, samples were examined using a JEOL JSM-IT500HR Field Emission Scanning Electron Microscope coupled with Oxford X-Max 150 Energy Dispersive System (FESEM-EDS).

### 2.2. Data treatment

Rainfall data were obtained from a rain gauge station located at the Odiel River basin (at El Campillo, about 8 km from OD2), and flow information was acquired from the stream gauge station at OD4 (Sotiel Coronada) (Fig. 1), all belonging to the monitoring network of the Andalusian Government. The net acidity (NA) in samples was determined according to Kirby and Cravotta (2005) (which include proton concentration and hydrolysable elements such as Fe, Al and Mn), modified to consider other hydrolysable elements commonly found in AMD such as Cu, Zn, Co and Ni.

For comparison purposes, chemical data were obtained from biomass ash (Table SM1), which may be analogue to the wildfire-ash produced in the wildfire. This material comes from the combustion of local agro-forestry biomass (mostly eucalyptus or mixtures) to produce electricity in a close power plant. Even though the formation conditions of both ash types may be different, since biomass ash is created in a controlled environment (Wang et al., 2012) and wildfire conditions strongly vary in time and space (Bodí et al., 2014), biomass ash effects on water and soil can be considered similar to those of wildfire-ash (Hannam et al., 2019). The collected ash is mainly composed of $SiO_2$ (69.3 wt%), $Al_2O_3$ (11.42 wt%), CaO (7.98 wt%), $K_2O$ (4.44 wt%), $Fe_2O_3$ (4.80 wt%), MgO (1.23 wt%), and to a lesser extent other elements such as Na (2.45 g/kg), P (1.67 g/kg), Ba (0.22 g/kg), S (0.20 g/kg) and Sr (0.19 g/kg), among others. In a pH paste test (solid-liquid ratio 1:2) performed to this material, pH values rise up to 12 and the alkalinity generated is more than 1000 mg/L of $CaCO_3$ equivalent.

Hydrochemical data prior to the wildfire are also available for the Odiel River in 2015 and 2016 at OD2, upstream of OD2 and the Agrio Creek (Table SM2), which joins the river between both points. This temporal dataset represents a range of relative contributions of the Odiel River and Agrio Creek upon different hydrological conditions, however only those corresponding to the same period (before and after the first rainfalls) were considered, so that chemical water quality of the river before and after the wildfire could be compared.

Saturation indices of waters with respect to some minerals commonly precipitated in AMD-affected systems were calculated using the PHREEQC code v3.7 (Parkhurst and Appelo, 2013) with WATEQ4f thermodynamic database (Ball and Nordstrom, 1991). The database was expanded with thermodynamic information for some mineral phases contained in the ash (mostly carbonates and oxides of Ca, K, Mg and Na; such as calcite, lime, periclase, sylvite, among others), as well as with equilibrium constants of schwertmannite from different authors (Bigham et al., 1996; Yu et al., 1999; Sánchez-España et al., 2011).

## 3. Results and discussion

### 3.1. Response of the river flow to rainfalls

The number of weather stations in the Odiel River watershed is limited, however complete information for the study period was

obtained from a gauge and a pluviometric station (Fig. SM1). As can be seen in Figure SM1, a fast response of river flow is observed upon the rainfall collected in the catchment. Thus, four main rainy episodes can be identified; the first commenced on September 18th with 9.4 mm recorded, which led to a slight increase in river flow of around 0.05 $m^3/s$ (Fig. SM1). The second episode recorded 49.8 mm on October 20th, increasing the river flow to around 3.77 $m^3/s$ (Fig. SM1). The third and fourth episodes occurred on November 5th and 25th with 17.4 and 33.6 mm leading to flow rises of up to 2.02 and 19.7 $m^3/s$, respectively (Fig. SM1).

The watercourses within the Odiel River basin commonly show very rapid flow responses to rainfall events due to the low permeability of their materials (Olías et al., 2006; Cánovas et al., 2007). The increase in humidity of catchment soils with persisting rainy episodes makes that the highest river flow is reached with lower amounts of rainfalls (Olías et al., 2006). The common response of river flow may be enhanced by increased runoff generation, induced by wildfire-ash clogging soil pores (Bodí et al., 2014), limiting more the infiltration capacity of these soils, or by loss of vegetation in the fire and its canopy interception, increasing net precipitation (Williams et al., 2019). Generally, this could potentially increase the erosion of soils and ash delivered to the streams. In Mediterranean climate, rainfalls are scarce over time and take place in short periods (within a few days or hours), mainly distributed along the wet season (September to March). However, this pattern may change since climate models predict the strengthening of these cycles (e.g., Giorgi and Lionello, 2008; Gianakopoulos et al., 2009)

### 3.2. *Temporal evolution of the hydrochemistry*

The hydrochemistry results of the sampling points OD2, OD3 and OD4 can be seen in Tables SM3, SM4 and SM5, respectively. The pH values during the study period varied between 2.3 and 3.5, with occasional rises to almost 5 downstream of the burnt areas. Electrical conductivity values fluctuated drastically throughout the sampling period. OD2 maximum values reached 17.77 mS/cm and minimum values came close to 1 mS/cm, with sharp variations along the temporal series (Fig. 2A). OD3 and OD4 showed EC values ranging from 2 to 4 mS/cm, with punctual maximums and minimums (7.02 and 5.86 mS/cm of maximum, respectively; and 0.42 mS/cm of minimum for both points; Fig. 2C and E).

The response of the parameters to the first rainfalls was unexpected for the three sites, given the previously reported behavior of the Odiel watershed in such events, with sharp increases in dissolved elements and decrease in pH values during the first rainfalls after summer (Cánovas et al., 2007; Sarmiento et al., 2009, 2017). There is a significant drop in EC (from 17.77 to 10.65 mS/cm at OD2 and from 3.74 to 1.97 mS/cm at OD4) due to a general decrease in dissolved metals concentrations, accompanied by a small increase in pH values at the sampling points

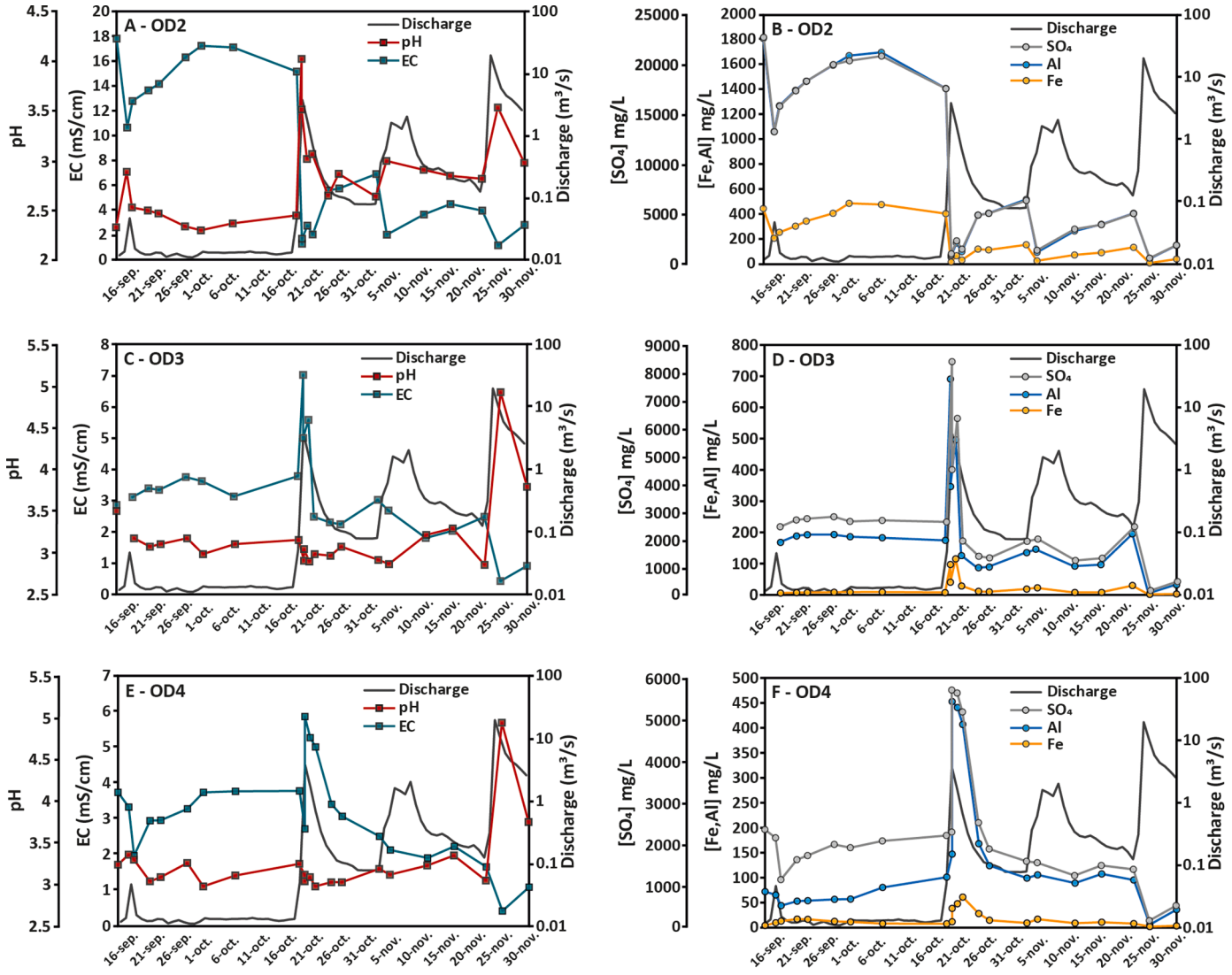


**Fig. 2.** Electrical conductivity (EC), pH, streamflow and evolution of the concentrations of Fe, Al and SO4 through the sampling period.

(from 2.32 to 2.88 at OD2 and from 3.24 to 3.36 at OD4), coinciding with the first rains and their fast response in the river flow (Fig. 2A, C and E). Unfortunately, there is missing data in OD3 coinciding with the first flow increment, however, the trend seems to be quite similar to OD4 response.

Almost all major element concentrations underwent a drastic drop in OD2 (Fe: from 443 to 205 mg/L; Al: 1805 to 1059 mg/L; sulfate: 22,760 to 13,296 mg/L) (Fig. 2B), resulting in a sharp decrease for net acidity, from an initial value of 12.1 to 7.01 g/L $CaCO_3$ eq. after the first rains (Table SM3). On the other hand, concentrations in OD3 and OD4 remained relatively constant, although there is a slight fall in Al and sulfate concentrations in OD4 (Fig. 2F). All elements behaved similarly during these rainfalls except for K, and to a lesser extent Ca and Na. Potassium concentration underwent an important rise in OD2 (from 1.11 to 10.3 mg/L), while Ca and Na suffered a slight decrease compared to the rest of dissolved elements. A few days after the rainy event, the physicochemical parameters and concentrations returned to their original pre-rain values (Fig. 2).

This behavior differs from the typical response of AMD-affected streams in semiarid catchments, when a notable increase in most elements associated with AMD is observed, either by the washing out of soluble salts accumulated along the riverbanks during the long dry season or by a higher contribution of AMD discharges to the river compared to that of runoff water (e.g., Johnson and Thornton, 1987; Keith et al., 2001; Cánovas et al., 2008). Previous studies on the water composition of the Odiel and Tinto River watersheds show fast and notable increases in EC at the onset of discharge rises during the first rain events, with increased concentrations for most elements related to AMD (e.g., Sarmiento et al., 2009; Cánovas et al., 2017; Olías et al., 2020). The influence of the alkaline ash, generated by the wildfire and its subsequent washout by run-off, may have attenuated the typical behavior of the Odiel River after the dry season, causing the precipitation of mineral phases and thus, decreasing the metal content in the water.

The second river flow increase, significantly larger than the first one (from 0.05 to 3.77 $m^3/s$), led to an extreme decrease in EC values at OD2 (from 15.15 to 1.28 mS/cm), concomitant with a pH rise of up to 4 (Fig. 2A). On the contrary, the opposite tendency was observed in OD3 and OD4, exhibiting the typical response of a watercourse affected by AMD (Fig. 2C and E). Due to the dissolution of evaporitic salts containing high amounts of toxic elements and acidity, EC increased (from 3.78 in both sites to 7.02 and 5.86 mS/cm, respectively) while pH declined slightly (from 3.16 and 3.25 to 2.91 and 3.04, respectively), coinciding with a maximum flow rate (3.77 $m^3/s$ at OD4).

This second event exhibited the largest decrease in acidity (Table SM3), sulfate and most metal concentrations in OD2 (Fig. 2B), with decreases ranging from 96% for acidity (down to 0.36 g/L $CaCO_3$ eq.) to more than 90% for major elements (Fe: from 402 to 10.2 mg/L; Al: from 1404 to 52.7 mg/L; sulfate: 17,599 to 863 mg/L). Otherwise, the decrease in Ca and Na concentrations was not so marked (26% and 31% in the first event, and 83% and 62% in this second event, respectively) while a slight increase in K concentration was observed (from 3.11 to 3.90 mg/L) compared to the first event. As mentioned before, a significant increase in concentrations was recorded in OD3 and OD4 (Fig. 2D and F) during these rainfalls, contrasting with the upstream sampling point. Net acidity increased from average values of 1200 mg/L to 4500 mg/L at OD3 (Table SM4) and 500 to 2900 mg/L $CaCO_3$ eq. at OD4 (Table SM5), probably by the intense washout of metal-rich efflorescent salts which remained in the riverbanks. It is striking that this pollution increase was registered in these last sampling points (OD3 and OD4) but not at the upstream most wildfire-affected one (OD2).

This indicates a different dominant process acting along the studied river reach. If the second event at OD2 would be only controlled by dilution, all dissolved concentrations would have undergone similar reduction percentages. As stated before, this is not the case for K, Ca and Na which behavior may suggest the influence of the wildfire-ash dissolution. On the contrary, at OD3 and OD4 located farther from fire-affected areas, no available ash may have been deposited, and the predominant process may have been the washout of efflorescent salts as well as the confluence of several AMD inputs in this river reach (Sarmiento et al., 2009). Moreover, considering that the main pollutant load delivered to the Odiel River comes from the Agrio Creek (Sánchez-España et al., 2005; Galván et al., 2016), which confluence is located upstream of OD2 (Fig. 1), is especially significant the substantial decrease in acidity, sulfate and metal concentrations observed in OD2 during both rain events, highlighting the powerful acidity attenuation capacity of wildfire-ash.

There were two additional flow rises in autumn 2020 (Fig. 2), nonetheless, the remaining acidity stored in the efflorescent salts may have diminished, as a consequence of intense dissolution processes in the prior rainfall events. In this sense, decreases in metal concentrations (277, 39.1 and 64.6 mg/L $CaCO_3$ eq. of net acidity for OD2, OD3 and OD4, respectively; Tables SM3, SM4 and SM5) in all sampling points and the highest pH values (3.53 in OD2 and 4.94 in both OD3 and OD4) were observed at the end of November 2020 (Fig. 2A, C and E).

### 3.3. Importance of efflorescent-salts washout in the river hydrogeochemistry

The evaporitic salts wash-out process predominantly controls the Odiel River hydrogeochemistry with the arrival of rainfall events after the dry season. In order to properly evaluate the consequences of this process together with the exceptional occurrence of the wildfire in the area, this section shows the evolution of some geochemical tracers during the sampling campaign.

Geochemical tracers are commonly used to identify and quantify geochemical reactions in aquatic systems. For example, the $Fe/SO_4$ ratio has been used to quantify the importance of pyrite oxidation, Fe secondary mineral precipitation and evaporitic sulfate salts dissolution in AMD-affected systems (e.g., Buckby et al., 2003; Cánovas et al., 2010). Thus, the $Fe/SO_4$ ratio in evaporitic sulfate salts or in Fe secondary minerals precipitated along riverbanks is higher than in the Odiel River waters since iron content in these precipitates is much higher than sulfate content (Cánovas et al., 2007; 2010). Then, dissolution of Fe-sulfate-rich salts may provoke a rise in the river water ratios and this can be used to determine whether the rainy events recorded in this study may have caused the dissolution of efflorescent salts, or even if other processes (such as dilution or ash flushing) have played a major role in water chemistry variations. Fig. 3A shows a decrease in $Fe/SO_4$ ratio at OD2 during the first rainy event, while the opposite trend is observed at OD4, a sampling point located downstream. This could be explained by the alkalinity contribution of the wildfire-ash to the water at OD2, which is the most fire-affected location. Alkalinity rises the pH and contributes to the precipitation of secondary Fe oxyhydroxysulfates during this discharge rise lowering the ratio, as explained before. The ratio rise at OD4 evidenced the salts flushing which may be attenuated by alkalinity running downstream given that metal and sulfate concentrations during the first event remained relatively constant or underwent slight decreases (Fig. 2F).

The increase in discharge during the second rainy event caused a strong decrease in $Fe/SO_4$ ratios at OD2 and increasing ones in both OD3 and OD4 (Fig. 3A). A major ratio peak occurs during the baseflow recession curve for the three sampling points (Fig. 3A). In this event, the hydrochemistry at OD2 would be controlled, firstly, by run-off dilution (i.e., mixing with freshwaters) and the relative predominance of wildfire-ash over soluble salts dissolution. Thus, the dissolution of remaining wildfire-ash would provide additional alkalinity, evidenced by an initial sharp decrease in the ratio caused by Fe precipitation, coinciding with a slight pH rise on October 21st (Fig. 2A), followed by an important increase in the ratio due to the dissolution of Fe-sulfate salts (Fig. 2A). Both OD3 and OD4 may have suffered preferentially salts washout processes explained by the progressive increase in $Fe/SO_4$

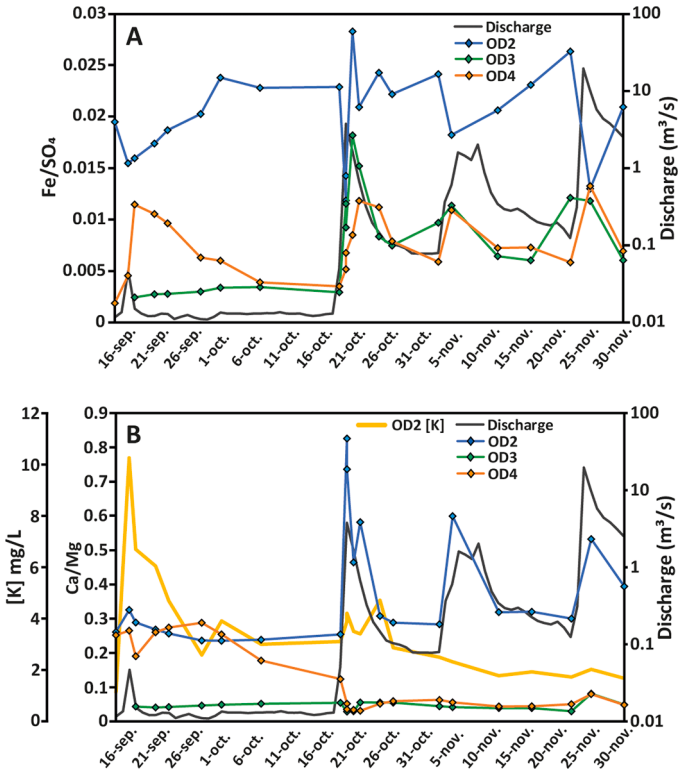


**Fig. 3.** (A) Fe/$SO_4$ and (B) Ca/Mg ratios during the considered study period. Dissolved K concentration is also shown in (B) for comparison purposes.

ratios along the second event (Fig. 3A), with no apparent influence of the wildfire-ash.

The last rainy events are initially characterized by a slight rise in the ratio within the rising limb for both OD3 and OD4, after the dissolution of residual amounts of efflorescent salts, followed by remarkable decrease in Fe/$SO_4$ ratios (Fig. 3A), due to precipitation processes of Fe oxyhydroxysulfates. On the contrary, OD2 ratios decreased, evidencing precipitation processes of Fe, probably influenced by wildfire-ash. This is supported by the behavior exhibited by pH and EC during these events (Fig. 2).

The plotting of Ca/Mg ratios can also provide valuable insights into predominant geochemical processes during the study period. Efflorescent salts are commonly richer in Mg than in Ca and typically this ratio may be higher in the Odiel River during the dry season due to important evaporitic sulfate precipitation processes and decreasing during the first rainfalls of autumn as a consequence of the salts flush out (Cánovas et al., 2007). The first rise in flow rate shows an evident increase in Ca/Mg at OD2 and to a lesser extent at OD4, followed by fast drop in the ratio (Fig. 3B). This response agrees well with the Fe/$SO_4$ ratios evolution, since the effect of the efflorescent salts washout may have been neutralized in OD2 and initially attenuated in OD4 because of the alkalinity provided by the wildfire-ash dissolution within the first rainfall event. The second event hydrochemistry at OD2 may be still influenced by ash dissolution, while at OD3 and OD4 it should be fully controlled by evaporitic salts dissolution. A similar behavior of Ca/Mg to previous Fe/$SO_4$ ratios in the second event (Fig. 3A) supports this interpretation. Besides, potassium concentration peaks in OD2 (Fig. 3B), coinciding with precipitation/neutralization evidenced by Fe/$SO_4$ and Ca/Mg ratios, highlight the remarkable role played by wildfire-ash on the river hydrochemistry.

The Ca/Mg ratio during the last rainfalls assist in evaluating whether dilution processes are the main factor or there are other factors implied in the hydrochemistry evolution. Constant ratios at OD3 and OD4 suggest dilution, contrasting the second event ruled by the evaporitic salts washout. However, at the upstream point of OD2, the ratio systematically increases as did in previous events. The same case occurs for the Na/$SO_4$ ratio (Fig. SM2) Then, it is possible that the wildfire-ash have controlled the entire temporal series of OD2, along with the typical processes occurring in AMD-waters.

### 3.4. *Importance of the dissolution of wildfire-ash in the river hydrogeochemistry*

Calcium (Ca), magnesium (Mg), sodium (Na) and potassium (K) are common elements of wildfire-ash, in which they usually occur as easily leachable mineral species (Ulery et al., 1993; Bodí et al., 2014; Pereira et al., 2014). Calcium concentrations decrease during the first and second rainy events in OD2, as well as most major AMD elements (around 40% for AMD elements and 25% for Ca in OD2 first event; and around 95% and 80%, respectively, in OD2 second event). Despite that it is expected that some amounts of Ca may come from the dissolution of the wildfire-ash, given that Ca is a major component of them, and its decrease in concentration is attenuated compared to other AMD-elements in OD2. This also happens for Na, which decreases accounts for 30% and 60% in the 1st and 2nd events respectively. On the other hand, K shows sudden increases in each discharge peak (Fig. 3B).

In an effort to check if the concentrations of these elements in the Odiel River are mainly supplied or affected by wildfire-ash washout, different end-members are represented in Fig. 4: a) biomass ash (an analogue to wildfire-ash), b) Odiel River waters prior to the Agrio Creek confluence, c) the Agrio Creek, and d) Odiel River after the confluence between Odiel River and Agrio Creek, where OD2 is located (Cinco Ojos Bridge in Fig. 1). Generally, normal patterns of K concentrations in the Odiel River show maximum values during summer and minimum in autumn (Cánovas et al., 2007), coinciding with the first rainfalls after the dry season. The solubility of K in AMD environments is commonly controlled by jarosite precipitation (Accornero et al., 2005). However, during the rainy events in OD2 there is a remarkable increase in K concentrations. An evolution of K concentration during and after the first rains towards the extreme member of the biomass ash composition is observed. This trend is observed not only in the plotting between K-S (Fig. 4), but also in Ca-K and Na-K (Fig. SM3).

The Odiel River waters have very similar relationships between K and S contents (Fig. 4), suggesting that dilution (and mixing) processes between AMD-affected and unaffected waters may control the solubility of both elements. OD2 Pre-rain sample in Fig. 4 represent concentrations of K-S (Ca-K and Na-K in Fig. SM3) before the first rainfall of the sampling period, when the Agrio Creek discharge was the main water contributor to the Odiel River during the summer. OD2 1st Rain group shows the evolution of these elements during the first discharge rise. As can be seen, K in these samples moves towards the extreme member of

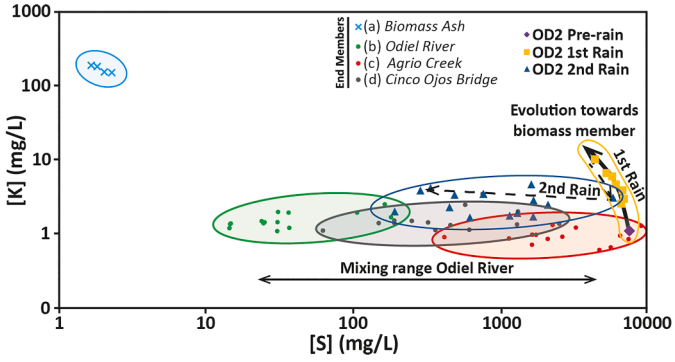


**Fig. 4.** Potassium concentration as a hydrogeochemical tracer of the wildfire-ash influence in the Odiel River. Extreme members are represented in order to compare the behavior of K during these events after the wildfire and a common hydrological year.

the biomass ash (Fig. 4) (also Ca-K and Na-K, Fig. SM3), instead of following a pattern of dilution over the shown trend of the Odiel River extreme members. In addition, an increasing release of elements contained in wildfire-ash was observed as in ash leaching experiments carried out by Audry et al. (2014), which reported a preferential release of elements ($K > Mg > Na > Si > Ca$). Thus, a quick release of K and to a lesser extent Ca and Na contained in the ash was observed within the first event, probably due to a higher solubility of the K mineral phases. Moreover, the major K peak also coincided with the unusual behavior of $Fe/SO_4$ and Ca/Mg ratios showed in Fig. 3, so there are multiple lines of evidence supporting that the first event is controlled by wildfire-ash washout.

OD2 2nd Rain group follows the normal trend of the Odiel River extreme members, nevertheless a slight influence of the biomass ash member is observed (Fig. 4). Ca and Na concentrations also reveal such influence (see Fig. SM4), given that Ca/Fe and Na/Fe ratios increased during the second rainfall (also Ca/Mg in Fig. 3B and $Na/SO_4$ in Fig. SM2), concomitant with minor decreases in concentrations compared to other major AMD-elements. These ratios are higher than those expected upon predominance of dilution processes, evidencing the probable dissolution of the less soluble phases richer in Ca and Na contained in the wildfire-ash, which could not be dissolved during the first rain. Ash leaching experiments reported by Audry et al. (2014) exhibited that Na is released before Ca. However, Ca/Fe values are much higher than Na/Fe ratio (Fig. SM4). Therefore, there should be a more significant input of Ca than Na due to a high Ca content in the wildfire-ash (Table SM1) leading to a major release of Ca than Na (see also Ca/Na ratios in Fig. SM4), concurring with the elements dissolution rates calculated by Audry et al. (2014). Johnston and Maher (2022) also reported a similar order in elevated concentrations of K, Ca and Na.

In summary, there is a quick release of K within the first rain event, contained in the most soluble phases of the wildfire-ash, with a lesser dissolution of Ca and Na phases, resulting in an increase of K concentration in the Odiel River. The second event, with a larger increment in run-off, causes the flush out of the less soluble phases richer in Ca and Na, modifying the typical trend during dilution processes and changing the ratios during the second rainfall. This is also demonstrated in Concentration-Discharge hysteresis curves in Fig. SM5, contrasting previously published hysteresis curves for the AMD context (Cánovas et al., 2010).

Samples collected during the last rainy events exhibited similar relationships between K and S (and other elements) than those typical of the Odiel River, which obeys to common dilution processes in this watercourse. However, Ca/Mg (Fig. 3B) and $Na/SO_4$ (Fig. SM2) ratios evidence that Ca and Na concentrations in the river are still slightly influenced by wildfire-ash dissolution. Although Si and Mg are also major components of wildfire-ash, there seems to have no influence on the AMD hydrochemistry. Silicon must be likely hosted in silica phases which are very insoluble, whereas in the case of Mg, its high content in AMD may have masked the possible influence of the Mg contained in the wildfire-ash.

In order to confirm which mineral phases are precipitating/dissolving in the Odiel River during the rainy events, the saturation indices (SI) of phases commonly found in AMD environments (Sánchez España et al., 2005) have been calculated by PHREEQC. For simplicity purposes, only information in OD2, the most affected area by wildfire, will be discussed. Jarosite dissolution might be a source of potassium ($KFe_3(SO_4)_2(OH)_6$) as a result of pH increments during rainfalls, since jarosite group minerals are only stable at very acid conditions (Das et al., 1996). However, SI showed oversaturation for jarosite (ss) and K-jarosite during the whole event, concluding that no K is coming from the dissolution of jarosite (Table SM6).

Schwertmannite SI values depends greatly on the equilibrium constant used in PHREEQC calculations. Equilibrium constants proposed by Sánchez España et al. (2011) and Bigham et al. (1996) for schwertmannite provided SI values showing undersaturation conditions or close to equilibrium in OD2 (Table SM6). However, using the thermodynamic data from Yu et al. (1999), schwertmannite appears to be oversaturated in the whole temporal series (Table SM6). This concern is due to schwertmannite's metastable nature and its variable composition, largely affected by sulfate concentration in the water (Schoepfer and Burton, 2021). In a pe-pH predominance diagram for stable and metastable Fe mineral phases (Caraballo et al., 2013), all OD2 samples plot within the schwertmannite field (Fig. SM6), supporting that no jarosite may be precipitating, and oversaturation values are probably due to high K concentrations. Mineralogical evidences support this fact, since globular aggregates in samples were observed by FE-SEM in particulate matter retained in filters, which was composed mostly by iron and sulfur suggesting the presence of schwertmannite. Therefore, the mineral assemblage in filters was dominated by silicates, and Fe mineral phases with a morphology and chemical composition typical of schwertmannite, without a clear jarosite identification (Fig. 5).

Mineral ash portion is mainly constituted by silica, carbonates and oxides (Bodí et al., 2014). All K, Ca and Na carbonates, oxides and salts considered appear to be undersaturated in these waters (Table SM6) according to PHREEQC calculations. That is, they can be easily dissolved into the Odiel River waters and provide the alkalinity needed to attenuate the AMD pollution. Besides, SI estimations also support the element release order ($K > Mg > Na > Si > Ca$) observed in this study and previously reported by Audry et al. (2014), with the K phases having the most subsaturated values, expecting a quick dissolution of them, followed by Na and Ca phases. Since the second rainy event is of greater magnitude than the first one, the runoff generated may be enough to dissolve the remaining wildfire-ash rich in Ca and Na that were not previously washed during the first event due to its lower solubility. As expected, oxides were more subsaturated than carbonates and alkaline salts and should dissolve more easily from the ash.

### 3.5. Global implications of this study

Potassium, Ca and Na have been widely reported to be easily water-extractable elements from ash produced in Mediterranean regions (generated either in wildfires or laboratory experiments) (Ferreira et al., 2005; Úbeda et al., 2009; Pereira et al., 2012, 2014). Sequeira et al. (2020) observed increases in K, Ca and Na concentrations during the first rainy period after multiple fires occurred in Portugal in an area dominated by *Pinus pinaster*, also abundant in the study area. Pereira et al. (2011) reported similar responses in a *Quercus suber* forest located in the northeast of the Iberian Peninsula. Other studies in the same geographic context (Costa et al., 2014; Mansilha et al., 2017) showed high values of these elements as well as slight increases in pH and alkalinity. In these cases, changes in water pH, driven by ash leaching, could be buffered at pH near neutrality limiting the capacity of ash to increase the pH and alkalinity. On the contrary, the high reactivity of ash in AMD waters (higher solubility due to low pH values) could lead to a major influence in the water parameters, considering that Fe buffer occurs at pH 2.5–3.5 (Nordstrom and Alpers, 1999). These authors have also reported increases in other elements considered in fresh waters as trace elements, but their high concentrations in AMD do not allow a proper analysis. For example, Johnston and Mahor (2022) showed increases in concentrations following the order $K>Ca>SO_4>HCO_3\approx Mg>Cl>Na$. In the AMD context, some of these changes in concentrations would be lost in the AMD background because of its extreme concentrations of dissolved elements. Santín et al. (2015) reported a similar response in an Australian eucalypt forest fire comparable to the biomass ash used in this research for comparison purposes. Although, these chemical changes in water mostly depend on the composition of the ash generated and then flushed.

Wildfire-ash driven neutralization of OD2 acid waters was remarkable, with decreases in acidity for each rainfall event (Table SM3). Besides, this is a striking fact considering the huge acidity load provided by the Agrio Creek, upstream of OD2 (Galván et al., 2016) which may have

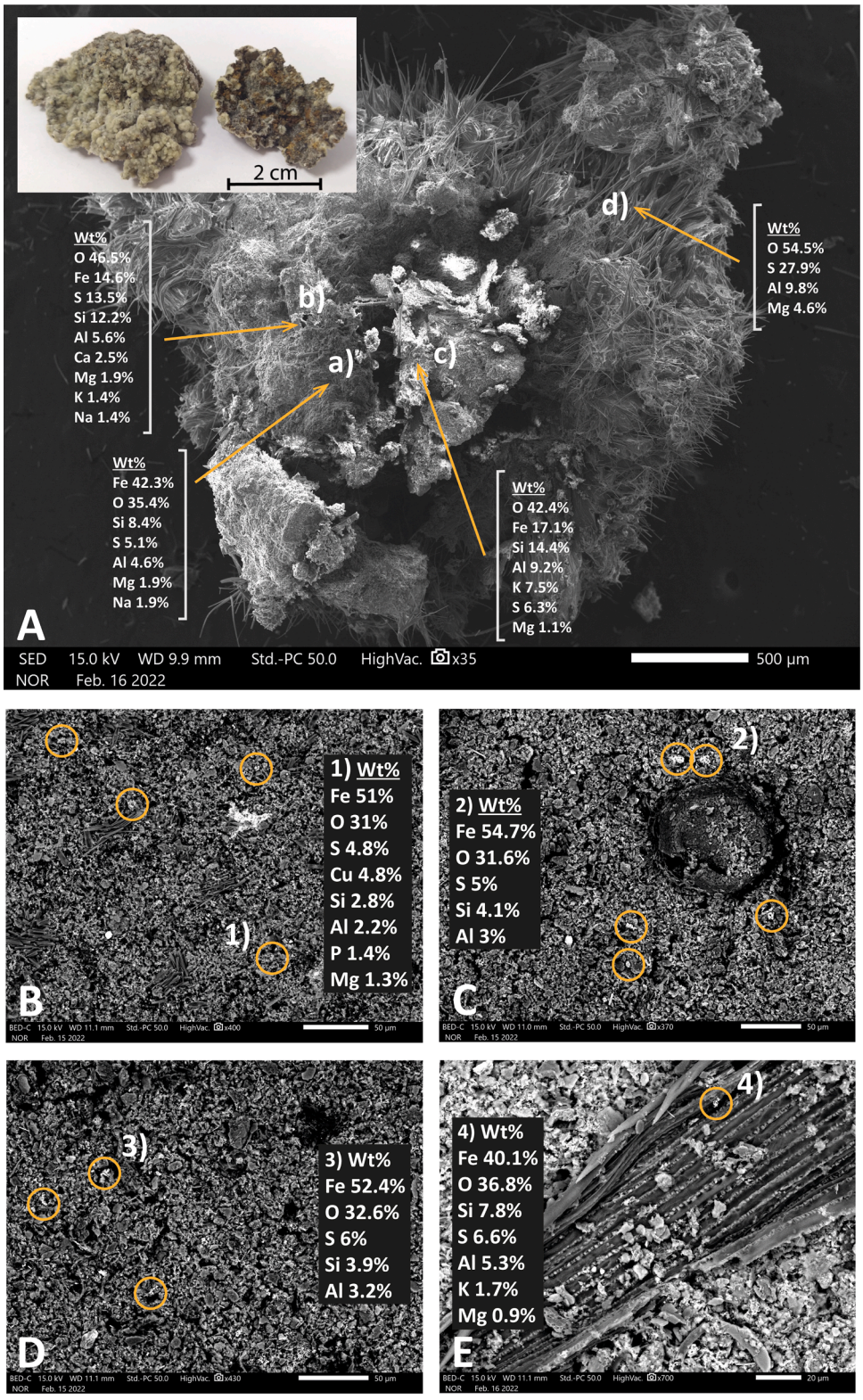


**Fig. 5.** (A): Secondary electron image of an ash particle with evaporitic salts. In the massive portion surrounding the clearer center zone, it has been suggested the presence of schwertmannite with some metals coprecipitated/adsorbed. Semi-quantitative composition shows the presence of K, Ca and Na, probably contained within the ash. (B), (C), (D) and (E): Backscattered electron images of particulate matter collected on September 18th. Globular schwertmannite has been identified (orange marks), dominating the silicates portion.

been neutralized by the ash dissolution, controlling the hydrogeochemistry of this portion of the Odiel River during the study period. Despite that, neutralization is only temporary, given that acid conditions are quickly recovered after the rain events, and may have occurred until all ashes have been dissolved. The watershed is intensely polluted by AMD with numerous leachates joining the main Odiel watercourse (Cánovas et al., 2021). That is why downstream (OD3 and OD4) the influence of ash dissolution plays a minor role and the hydrogeochemistry is mainly controlled by AMD and efflorescent salts washout. Overall, the wildfire-ash effects are restrained spatial and temporally by the strong load of acidity reaching the Odiel River. Nonetheless, it is expected that in smaller AMD-affected watercourses the same effects may be magnified. Even, in cases of AMD-affected water courses with low acidity concentration (e.g., coal mines or smaller

sulfide mines) (Lee et al., 2002; Cravotta, 2008), the neutralizing effects of wildfire-ash may be more significant and long-lasting.

In addition, a long-term response of AMD-affected catchments to wildfire may be the increase in the AMD generation rates. The loss of vegetation after the wildfire induces a greater water infiltration into waste mine dumps and adits, which function as anthropogenic aquifers (Caraballo et al., 2016), promoting the generation of AMD. Canopy interception decrease and overland flow increase after wildfires (Bodí et al., 2014; Williams et al., 2019), allowing the arrival of greater amounts of water to mine areas. In fact, Murphy et al. (2020) observed remobilization of arsenic and other metals from legacy mine waste to surface water due to greater run-off during post-fire rainfalls.

## 4. Conclusions

This is the first time that the direct consequences of a wildfire on an AMD-affected watercourse have been studied. The washout of wildfire-ash seems to counterbalance the usual behavior and patterns of the Odiel River hydrogeochemistry during autumn (i.e., dramatic increases in most elements, high EC and decreases in pH values as a result of soluble salts flushing), when the first rainfalls after the dry season are recorded. Due to the wildfire-ash washout and the subsequent input of alkalinity to the water during the first rainfalls of autumn 2020 (immediately after the wildfire), the acidifying effect of efflorescent salts flushing was somewhat neutralized. The neutralization was limited to fire-affected portions of the watercourse, contrary to downstream segments mainly controlled by common AMD processes.

The utilization of different methods commonly used in AMD to evaluate processes such as elemental ratios, end-members analysis or the drawing of hysteresis curves, combined with previously published information about wildfires consequences in terrestrial and aquatic systems, have shed light to the difficulty of conducting research in both AMD and wildfire topics. This will certainly allow to further anticipate the response of other AMD-affected water systems to wildfires in the global context of global warming, where existent models foresee an increased expectation in the number, severity and burnt area of wildfires associated to climate change.

## Declaration of Competing Interest

The authors declare that they have no known competing financial interests or personal relationships that could have appeared to influence the work reported in this paper.

## Data Availability

Data will be made available on request.

## Acknowledgements

This research was supported by the AIHODIEL project (PYC20 RE 032 UHU) within the 2020 call for grants for the implementation of projects of collaborative interest in the field of innovation ecosystems co-financed by the FEDER program in Andalucía for the period 2014–2020. Jonatan Romero is financed by a FPU program of the Spanish Ministry of Education of Vocational Training (FPU20/04441). C.R Cánovas thanks the Spanish Ministry of Science and Innovation for the Postdoctoral Fellowship granted under application reference RYC2019–027949-I. Funding for open access charge: Universidad de Huelva/CBUA. The authors gratefully appreciate the constructive comments and suggestions from the editor Mark van Loosdrecht and two anonymous reviewers.

## Supplementary materials

Supplementary material associated with this article can be found, in the online version, at doi:10.1016/j.watres.2023.119791.

## References

Accornero, M., Marini, L., Ottonello, G., Zuccolini, M.V., 2005. The fate of major constituents and chromium and other trace elements when acid waters from the derelict Libiola mine (Italy) are mixed with stream waters. Appl. Geochem. 20 (7), 1368–1390. https://doi.org/10.1016/j.apgeochem.2005.03.001.

Audry, S., Akerman, A., Riotte, J., Oliva, P., Maréchal, J.C., Fraysse, F., Pokrovsky, O.S., Braun, J.J., 2014. Contribution of forest fire ash and plant litter decay on stream dissolved composition in a sub-humid tropical watershed (Mule Hole, Southern India). Chem. Geol. 372, 144–161. https://doi.org/10.1016/j.chemgeo.2014.02.016.

Ball, J.W., Nordstrom, D.K., 1991. WATEQ4F – User's manual with revised thermodynamic data base and test cases for calculating speciation of major. Trace Redox Elements Nat. Waters. https://doi.org/10.3133/ofr90129.

Bigham, J.M., Schwertmann, U., Traina, S.J., Winland, R.L., Wolf, M., 1996. Schwertmannite and the chemical modeling of iron in acid sulfate waters. Geochim. Cosmochim. Acta 60 (12), 2111–2121. https://doi.org/10.1016/0016-7037(96)00091-9.

Bladon, K.D., Emelko, M.B., Silins, U., Stone, M., 2014. Wildfire and the future of water supply. Environ. Sci. Technol. 48, 8936–8943. https://doi.org/10.1021/es500130g.

Bodí, M.B., Martin, D.A., Balfour, V.N., Santín, C., Doerr, S.H., Pereira, P., Mataix-Solera, J., 2014. Wildland fire ash: production, composition and eco-hydro-geomorphic effects. Earth Sci. Rev. 130, 103–127. https://doi.org/10.1016/j.earscirev.2013.12.007.

Bogush, A.A., Dabu, C., Tikhova, V.D., Kim, J.K., Campos, L.C., 2020. Biomass ashes for acid mine drainage remediation. Waste Biomass Valorization 11 (9), 4977–4989. https://doi.org/10.1007/s12649-019-00804-9.

Buckby, T., Black, S., Coleman, M.L., Hodson, M.E., 2003. Fe-sulphate-rich evaporative mineral precipitates from the Rio Tinto, southwest Spain. Mineral. Mag. 67 (2), 263–278. https://doi.org/10.1180/0026461036720104.

Cánovas, C.R., Hubbard, C.G., Olías, M., Nieto, J.M., Black, S., Coleman, M.L., 2008. Hydrochemical variations and contaminant load in the Río Tinto (Spain) during flood events. J. Hydrol. (Amst.) 350 (1–2), 25–40. https://doi.org/10.1016/j.jhydrol.2007.11.022.

Cánovas, C.R., Macías, F., Basallote, M.D., Olías, M., Nieto, J.M., Pérez-López, R., 2021. Metal (loid) release from sulfide-rich wastes to the environment: the case of the Iberian Pyrite Belt (SW Spain). Curr. Opin. Environ. Sci. Health 20, 100240. https://doi.org/10.1016/j.coesh.2021.100240.

Cánovas, C.R., Macías, F., Olías, M., López, R.P., Nieto, J.M., 2017. Metal-fluxes characterization at a catchment scale: study of mixing processes and end-member analysis in the Meca River watershed (SW Spain). J. Hydrol. (Amst.) 550, 590–602. https://doi.org/10.1016/j.jhydrol.2017.05.037.

Cánovas, C.R., Olías, M., Nieto, J.M., Galván, L., 2010. Wash-out processes of evaporitic sulfate salts in the Tinto river: hydrogeochemical evolution and environmental impact. Appl. Geochem. 25 (2), 288–301. https://doi.org/10.1016/j.apgeochem.2009.11.014.

Cánovas, C.R., Olías, M., Nieto, J.M., Sarmiento, A.M., Cerón, J.C., 2007. Hydrogeochemical characteristics of the Tinto and Odiel Rivers (SW Spain). Factors controlling metal contents. Sci. Total Environ. 373 (1), 363–382. https://doi.org/10.1016/j.scitotenv.2006.11.022.

Cánovas, C.R., Olias, M., Sarmiento, A.M., Nieto, J.M., Galván, L., 2012. Pollutant transport processes in the Odiel River (SW Spain) during rain events. Water Resour. Res. (6), 48. https://doi.org/10.1029/2011WR011041.

Caraballo, M.A., Rimstidt, J.D., Macías, F., Nieto, J.M., Jr, Hochella, M, F, 2013. Metastability, nanocrystallinity and pseudo-solid solution effects on the understanding of schwertmannite solubility. Chem. Geol. 360, 22–31. https://doi.org/10.1016/j.chemgeo.2013.09.023.

Caraballo, M.A., Macías, F., Nieto, J.M., Ayora, C., 2016. Long term fluctuations of groundwater mine pollution in a sulfide mining district with dry Mediterranean climate: implications for water resources management and remediation. Sci. Total Environ. 539, 427–435.

Copernicus Emergency Management Service (© 2020 European Union), [EMSR457] Forest Fire in Almonaster La Real, Spain.

Costa, M.R., Calvão, A.R., Aranha, J., 2014. Linking wildfire effects on soil and water chemistry of the Marão River watershed, Portugal, and biomass changes detected from Landsat imagery. Appl. Geochem. 44, 93–102. https://doi.org/10.1016/j.apgeochem.2013.09.009.

Cravotta III, C.A., 2008. Dissolved metals and associated constituents in abandoned coal-mine discharges, Pennsylvania, USA. Part 1: constituent quantities and correlations. Appl. Geochem. 23 (2), 166–202.

Das, G.K., Acharya, S., Anand, S., Das, R.P., 1996. Jarosites: a review. Mineral Process. Extract. Metullarg. Rev. 16 (3), 185–210. https://doi.org/10.1080/08827509708914135.

Earl, S.R., Blinn, D.W., 2003. Effects of wildfire ash on water chemistry and biota in South-Western USA streams. Freshw. Biol. 48 (6), 1015–1030.

Emelko, M.B., Silins, U., Bladon, K.D., Stone, M., 2011. Implications of land disturbance on drinking water treatability in a changing climate: demonstrating the need for "source water supply and protection" strategies. Water Res. 45 (2), 461–472.

Emelko, M.B., Stone, M., Silins, U., Allin, D., Collins, A.L., Williams, C.H., Bladon, K.D., 2016. Sediment-phosphorus dynamics can shift aquatic ecology and cause downstream legacy effects after wildfire in large river systems. Glob. Chang. Biol. 22 (3), 1168–1184.

Emmerton, C.A., Cooke, C.A., Hustins, S., Silins, U., Emelko, M.B., Lewis, T., Kruk, M.K., Taube, N., Zhu, D., Jackson, B., Stone, M., Kerr, J.G., Orwin, J.F., 2020. Severe western Canadian wildfire affects water quality even at large basin scales. Water Res. 183, 116071 https://doi.org/10.1016/j.watres.2020.116071.

Ferreira, A.J.D., Coelho, C.O.A., Boulet, A.K., Lopes, F.P., 2005. Temporal patterns of solute loss following wildfires in Central Portugal. Int. J. Wildland Fire 14 (4), 401–412.

Gabet, E.J., Bookter, A., 2011. Physical, chemical and hydrological properties of Ponderosa pine ash. Int. J. Wildland Fire 20 (3), 443–452. https://doi.org/10.1071/WF09105.

Galván, L., Olías, M., Cánovas, C.R., Sarmiento, A.M., Nieto, J.M., 2016. Hydrological modeling of a watershed affected by acid mine drainage (Odiel River, SW Spain). Assessment of the pollutant contributing areas. J. Hydrol. (Amst) 540, 196–206. https://doi.org/10.1016/j.jhydrol.2016.06.005.

Giorgi, F., Lionello, P., 2008. Climate change projections for the Mediterranean region. Glob. Planet Change 63 (2–3), 90–104. https://doi.org/10.1016/j.gloplacha.2007.09.005.

Giannakopoulos, C., Le Sager, P., Bindi, M., Moriondo, M., Kostopoulou, E., Goodess, C. M, 2009. Climatic changes and associated impacts in the Mediterranean resulting from a 2 C global warming. Glob. Planet Change 68 (3), 209–224. https://doi.org/10.1016/j.gloplacha.2009.06.001.

Hannam, K.D., Fleming, R.L., Venier, L., Hazlett, P.W., 2019. Can bioenergy ash applications emulate the effects of wildfire on upland forest soil chemical properties? Soil Sci. Soc. Am. J. 83, S201–S217.

Johnson, C.A., Thornton, I., 1987. Hydrological and chemical factors controlling the concentrations of Fe, Cu, Zn and As in a river system contaminated by acid mine drainage. Water Res. 21 (3), 359–365. https://doi.org/10.1016/0043-1354(87)90216-8.

Johnston, S.G., Maher, D.T., 2022. Drought, megafires and flood-climate extreme impacts on catchment-scale river water quality on Australia's east coast. Water Res. 218, 118510.

Jolly, W.M., Cochrane, M.A., Freeborn, P.H., Holden, Z.A., Brown, T.J., Williamson, G.J., Bowman, D.M., 2015. Climate-induced variations in global wildfire danger from 1979 to 2013. Nat. Commun. 6 (1), 7537.

Keith, D.C., Runnells, D.D., Esposito, K.J., Chermak, J.A., Levy, D.B., Hannula, S.R., Watts, M., Hall, L., 2001. Geochemical models of the impact of acidic groundwater and evaporative sulfate salts on Boulder Creek at Iron Mountain, California. Appl. Geochem. 16 (7–8), 947–961. https://doi.org/10.1016/S0883-2927(00)00080-9.

Kinoshita, A.M., Chin, A., Simon, G.L., Briles, C., Hogue, T.S., O'Dowd, A.P., & Albornoz, A.U. (2016). Wildfire, water, and society: toward integrative research in the "Anthropocene". *Coastal Fluxes Anthropocene*, 16, 16–27. https://doi.org/10.1016/j.ancene.2016.09.001.

Kirby, C.S., Cravotta III, C.A, 2005. Net alkalinity and net acidity 1: theoretical considerations. Appl. Geochem. 20 (10), 1920–1940. https://doi.org/10.1016/j.apgeochem.2005.07.002.

Lee, G., Bigham, J.M., Faure, G., 2002. Removal of trace metals by coprecipitation with Fe, Al and Mn from natural waters contaminated with acid mine drainage in the Ducktown Mining District, Tennessee. Appl. Geochem. 17 (5), 569–581.

Macías, F., Pérez-López, R., Caraballo, M.A., Sarmiento, A.M., Cánovas, C.R., Nieto, J.M., Olías, M., Ayora, C, 2017. A geochemical approach to the restoration plans for the Odiel River basin (SW Spain), a watershed deeply polluted by acid mine drainage. Environ. Sci. Pollut. Res. Int. 24 (5), 4506–4516. https://doi.org/10.1007/s11356-016-8169-9.

Mansilha, C., Duarte, C.G., Melo, A., Ribeiro, J., Flores, D., Marques, J.E., 2017. Impact of wildfire on water quality in Caramulo Mountain ridge (Central Portugal). Sustain. Water Resour. Manag. 5 (1), 319–331. https://doi.org/10.1007/s40899-017-0171-y.

Millán-Becerro, R., Cáanovas, C.R., Pérez-López, R., Macías, F., Leon, R., 2021. Combined procedure of metal removal and recovery of technology elements from fertilizer industry effluents. J. Geochem. Explor. 221, 106698 https://doi.org/10.1016/j.gexplo.2020.106698.

Mishra, A., Alnahit, A., Campbell, B., 2021. Impact of land uses, drought, flood, wildfire, and cascading events on water quality and microbial communities: a review and analysis. J. Hydrol. (Amst.) 596, 125707.

Murphy, S.F., McCleskey, R.B., Martin, D.A., Holloway, J.M., Writer, J.H., 2020. Wildfire-driven changes in hydrology mobilize arsenic and metals from legacy mine waste. Sci. Total Environ. 743, 140635.

Nordstrom, D.K., Alpers, C.N., 1999. Geochemistry of acid mine waters. Environ. Geochem. Mineral Deposits 6, 133–160. October.

Nordstrom, D.K., Wilde, F.D., 1998. Reduction–oxidation potential (electrode method). National Field Manual for the Collection of Water Quality Data, book 9, chapter 6.5. US Geological Survey techniques of water-resources investigations, US Geological Survey, Reston, VA (20 pp.).

Nordstrom, D.K., Blowes, D.W., Ptacek, C.J., 2015. Hydrogeochemistry and microbiology of mine drainage: an update. Appl. Geochem. 57, 3–16. https://doi.org/10.1016/j.apgeochem.2015.02.008.

Olías, M., Cánovas, C.R., Basallote, M.D., Macías, F., Pérez-López, R., González, R.M., Millán-Becerro, R., Nieto, J.M., 2019. Causes and impacts of a mine water spill from an acidic pit lake (Iberian Pyrite Belt). Environ. Pollut. 250, 127–136. https://doi.org/10.1016/j.envpol.2019.04.011.

Olías, M., Cánovas, C.R., Macías, F., Basallote, M.D., Nieto, J.M., 2020. The evolution of pollutant concentrations in a river severely affected by acid mine drainage: Río Tinto (SW Spain). Minerals 10 (7), 598. https://doi.org/10.3390/min10070598.

Olías, M., Cánovas, C.R., Nieto, J.M., Sarmiento, A.M., 2006. Evaluation of the dissolved contaminant load transported by the Tinto and Odiel rivers (South West Spain). Appl. Geochem. 21 (10), 1733–1749.

Pacheco, F.A., Fernandes, L.F.S., 2021. Hydrology and stream water quality of fire-prone watersheds. Curr. Opin. Environ. Sci. Health 21, 100243. https://doi.org/10.1016/j.coesh.2021.100243nutri.

Parkhurst, D.L., Appelo, C.A.J., 2013. Description of input and examples for PHREEQC version 3—A computer program for speciation, batch-reaction, one-dimensional transport, and inverse geochemical calculations. US Geol. Surv. Techniques Methods 6, 497. https://doi.org/10.3133/tm6A43. A43.

Pausas, J.G., 2004. Changes in fire and climate in the eastern Iberian Peninsula (Mediterranean basin). Clim. Change 63 (3), 337–350. https://doi.org/10.1023/B:CLIM.0000018508.94901.9c.

Pereira, M.G., Trigo, R.M., da Camara, C.C., Pereira, J.M., Leite, S.M., 2005. Synoptic patterns associated with large summer forest fires in Portugal. Agric. For. Meteorol. 129 (1–2), 11–25. https://doi.org/10.1016/j.agrformet.2004.12.007.

Pereira, P., Úbeda, X., 2010. Spatial distribution of heavy metals released from ashes after a wildfire. J. Environ. Eng. Landsc. Manag. 18 (1), 13–22. https://doi.org/10.3846/jeelm.2010.02.

Pereira, P., Úbeda, X., Martin, D.A., 2012. Fire severity effects on ash chemical composition and water-extractable elements. Geoderma 191, 105–114. https://doi.org/10.1016/j.geoderma.2012.02.005.

Pereira, P., Úbeda, X., Martin, D., Mataix-Solera, J., Guerrero, C., 2011. Effects of a low severity prescribed fire on water-soluble elements in ash from a cork oak (Quercus suber) forest located in the northeast of the Iberian Peninsula. Environ. Res. 111 (2), 237–247.

Pereira, P., Ubeda, X., Martin, D., Mataix-Solera, J., Cerda, A., Burguet, M., 2014. Wildfire effects on extractable elements in ash from a Pinus pinaster forest in Portugal. Hydrol. Process. 28 (11), 3681–3690. https://doi.org/10.1002/hyp.9907.

Reale, J.K., Van Horn, D.J., Condon, K.E., Dahm, C.N., 2015. The effects of catastrophic wildfire on water quality along a river continuum. Freshw. Sci. 34 (4), 1426–1442.

Rust, A.J., Hogue, T.S., Saxe, S., McCray, J., 2018. Post-fire water-quality response in the western United States. Int. J. Wildland Fire 27 (3), 203–216.

Sánchez-España, J., Pamo, E.L., Santofimia, E., Aduvire, O., Reyes, J., Barettino, D., 2005. Acid mine drainage in the Iberian Pyrite Belt (Odiel river watershed, Huelva, SW Spain): geochemistry, mineralogy and environmental implications. Appl. Geochem. 20 (7), 1320–1356. https://doi.org/10.1016/j.apgeochem.2005.01.011.

Sánchez-España, J., Yusta, I., Diez-Ercilla, M., 2011. Schwertmannite and hydrobasaluminite: a re-evaluation of their solubility and control on the iron and aluminium concentration in acidic pit lakes. Appl. Geochem. 26 (9–10), 1752–1774. https://doi.org/10.1016/j.apgeochem.2011.06.020.

Santín, C., Doerr, S.H., Otero, X.L., Chafer, C.J., 2015. Quantity, composition and water contamination potential of ash produced under different wildfire severities. Environ. Res. 142, 297–308.

Sarmiento, A.M., Nieto, J.M., Olías, M., Cánovas, C.R., 2009. Hydrochemical characteristics and seasonal influence on the pollution by acid mine drainage in the Odiel River Basin (SW Spain). Appl. Geochem. 24 (4), 697–714. https://doi.org/10.1016/j.apgeochem.2008.12.025.

Schoepfer, V.A., Burton, E.D., 2021. Schwertmannite: a review of its occurrence, formation, structure, stability and interactions with oxyanions. Earth Sci. Rev. 221, 103811 https://doi.org/10.1016/j.earscirev.2021.103811.

Sequeira, M.D., Castilho, A.M., Dinis, P.A., Tavares, A.O., 2020. Impact assessment and geochemical background analysis of surface water quality of catchments affected by the 2017 Portugal Wildfires. Water (Basel) 12 (10), 2742. https://doi.org/10.3390/w12102742.

Smith, H.G., Sheridan, G.J., Lane, P.N., Nyman, P., Haydon, S., 2011. Wildfire effects on water quality in forest catchments: a review with implications for water supply. J. Hydrol. (Amst.) 396 (1–2), 170–192. https://doi.org/10.1016/j.jhydrol.2010.10.043.

Úbeda, X., Pereira, P., Outeiro, L., Martin, D.A., 2009. Effects of fire temperature on the physical and chemical characteristics of the ash from two plots of cork oak (Quercus suber). Land Degrad. Dev. 20 (6), 589–608. https://doi.org/10.1002/ldr.930.

Ulery, A.L., Graham, R.C., Amrhein, C., 1993. Wood-ash composition and soil pH following intense burning. Soil Sci. 156 (5), 358–364. https://doi.org/10.1097/00010694-199311000-00008.

Wang, L., Hustad, J.E., Skreiberg, Ø., Skjevrak, G., Grønli, M., 2012. A critical review on additives to reduce ash related operation problems in biomass combustion applications. Energy Procedia 20, 20–29.

Wang, X., Jiang, H., Fang, D., Liang, J., Zhou, L., 2019. A novel approach to rapidly purify acid mine drainage through chemically forming schwertmannite followed by lime neutralization. Water Res. 151, 515–522. https://doi.org/10.1016/j.watres.2018.12.052.

Williams, C.H., Silins, U., Spencer, S.A., Wagner, M.J., Stone, M., Emelko, M.B., 2019. Net precipitation in burned and unburned subalpine forest stands after wildfire in the northern Rocky Mountains. Int. J. Wildland Fire 28 (10), 750–760.

Younger, P., 1997. The longevity of minewater pollution: a basis for decision making. *Sci. Total Environ.* 194–195 (96), 457–466. https://doi.org/10.1016/S0048-9697,05383-1.

Yu, J.Y., Heo, B., Choi, I.K., Cho, J.P., Chang, H.W., 1999. Apparent solubilities of schwertmannite and ferrihydrite in natural stream waters polluted by mine drainage. Geochim. Cosmochim. Acta 63 (19–20), 3407–3416. https://doi.org/10.1016/S0016-7037(99)00261-6.